Supporting Information

Structural, Surface and Optical Properties of Transition Metal Doped Pyrite Thin Films by Aerosol-Assisted Chemical Vapour Deposition.

Sadia Khalid,[a,b,c] M. Azad Malik*[a], David J. Lewis[a,d], Ejaz Ahmed[b], Punjara Kevin,[d] Yaqoob Khan[c], Paul O'Brie[a,d]

[a]School of Materials, The University of Manchester, Oxford Road, Manchester, M13 9PL, U.K..
[b]Department of Physics, BahauddinZakariya University, Multan 60800, Pakistan.
[c]Nanoscience and Catalysis Division, National Centre for Physics, Quaid-i-Azam University Campus, Islamabad, 45320- Pakistan
[d]School of Chemistry, The University of Manchester, Oxford Road, Manchester, M13 9PL, U.K..

Corresponding Author
Dr. Mohammed Azad Malik.
Email: azad.malik@manchester.ac.uk.

Tel: +44 161 275 4653.
Fax: +44 161 275 4616.

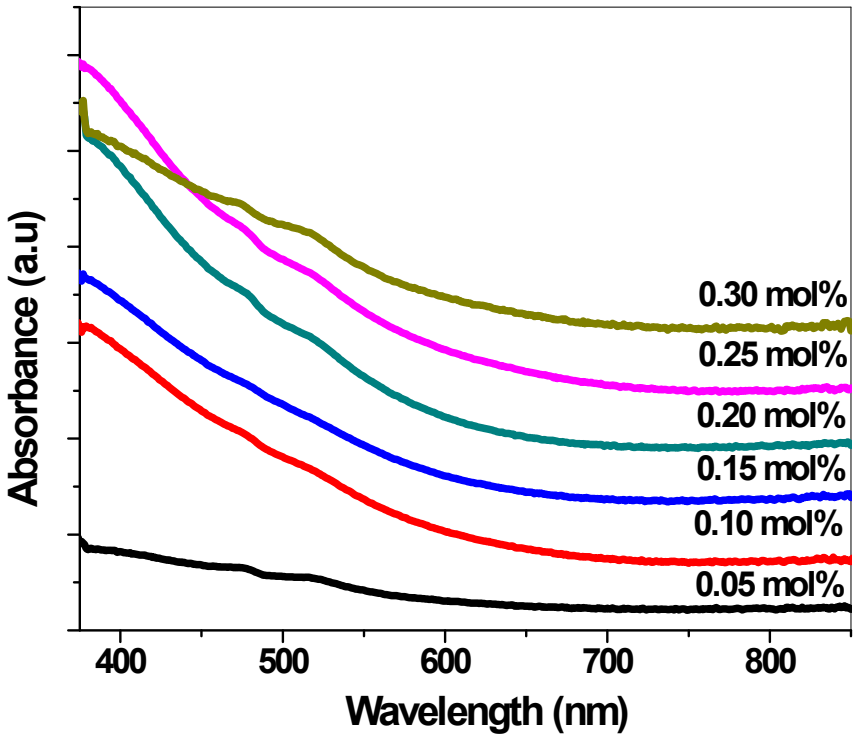

Figure S1. Visible absorbance spectra of cobalt doped pyrite $Co_xFe_{1-x}S_2$ thin films deposited from complexes (1) and (2) at 350 °C on glass substrate synthesized by AACVD with different starting ratio of cobalt complex (2).

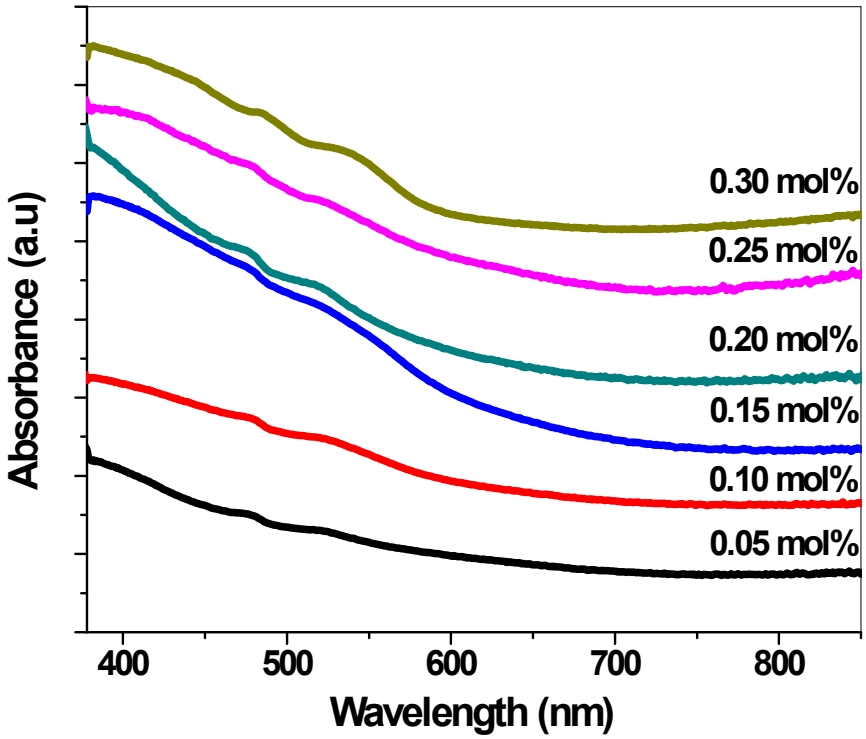

Figure S2. Visible absorbance spectra of nickel doped pyrite $Ni_xFe_{1-x}S_2$ thin films deposited from complexes (1) and (3) at 350 °C on glass substrate synthesized by AACVD with different starting ratio of nickel complex (3).

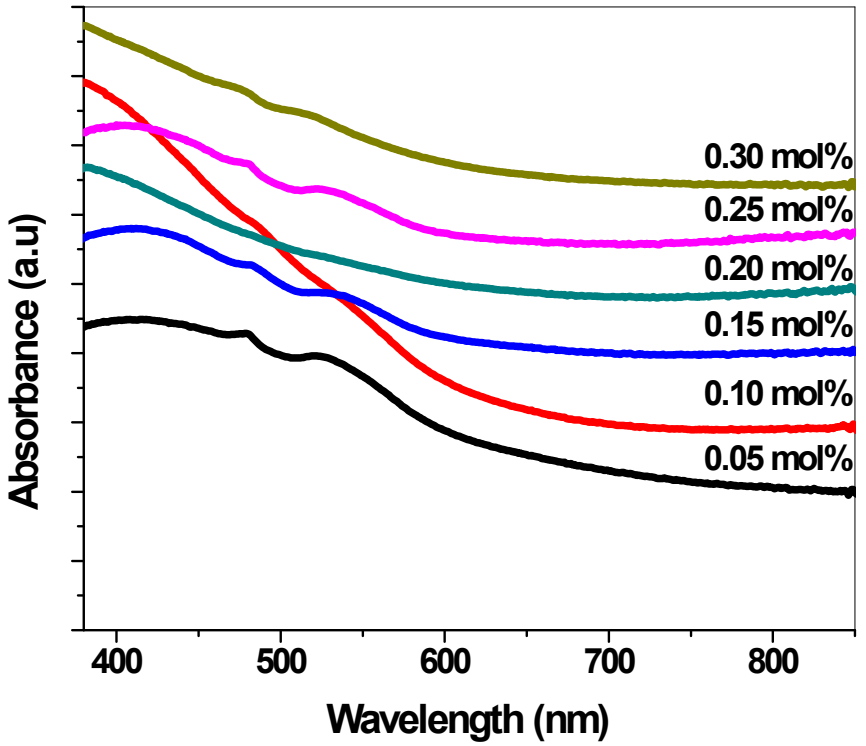

Figure S3. Visible absorbance spectra of copper-doped pyrite $Cu_xFe_{1-x}S_2$ thin films deposited from complexes (1) and (4) at 350 °C on glass substrate synthesized by AACVD with different starting ratio of copper complex (4)

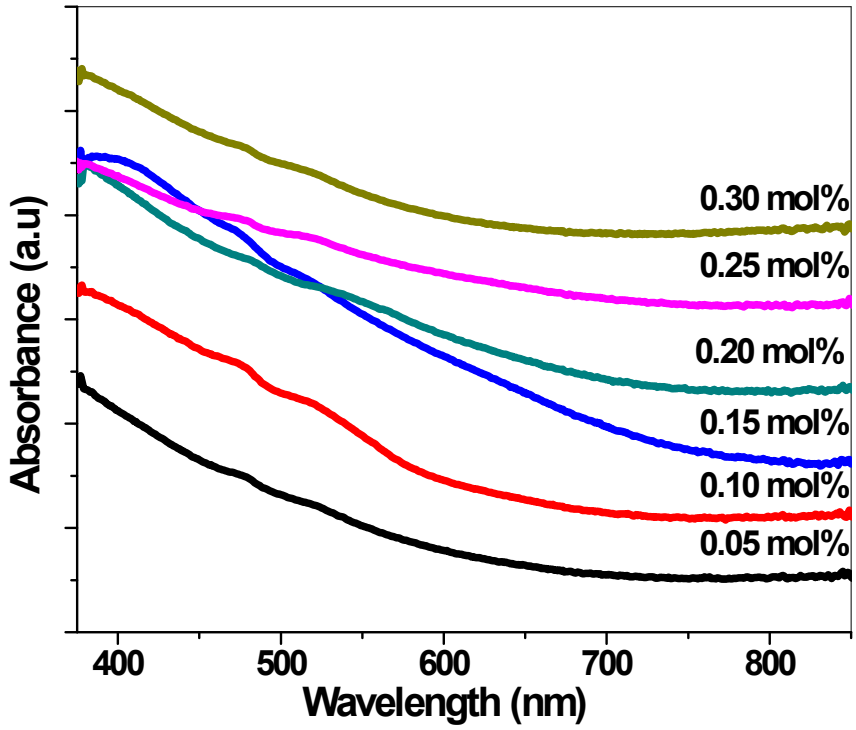

Figure S4. Absorbance spectra of zinc-doped pyrite $Zn_xFe_{1-x}S_2$ thin films deposited from complexes (1) and (5) at 350 °C on glass substrate synthesized by AACVD with different starting ratio of zinc complex (5)

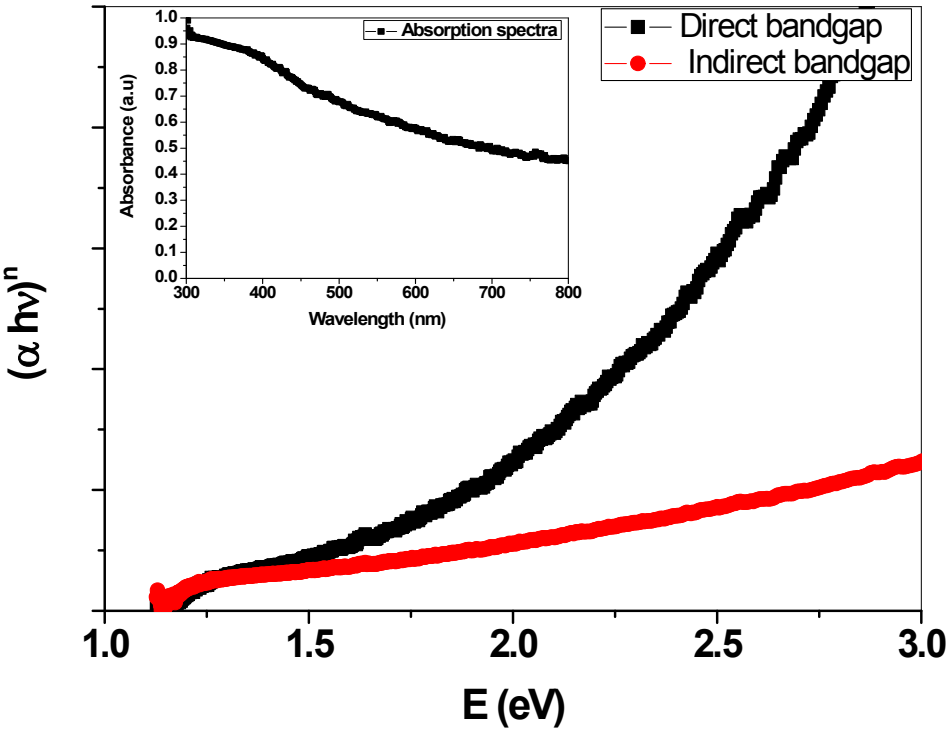

Figure S5 Direct (n = 2) and indirect (n = 1/2) band gap of iron sulphide thin films deposited from complexes (1) at 350 °C on glass substrate synthesised by AACVD.

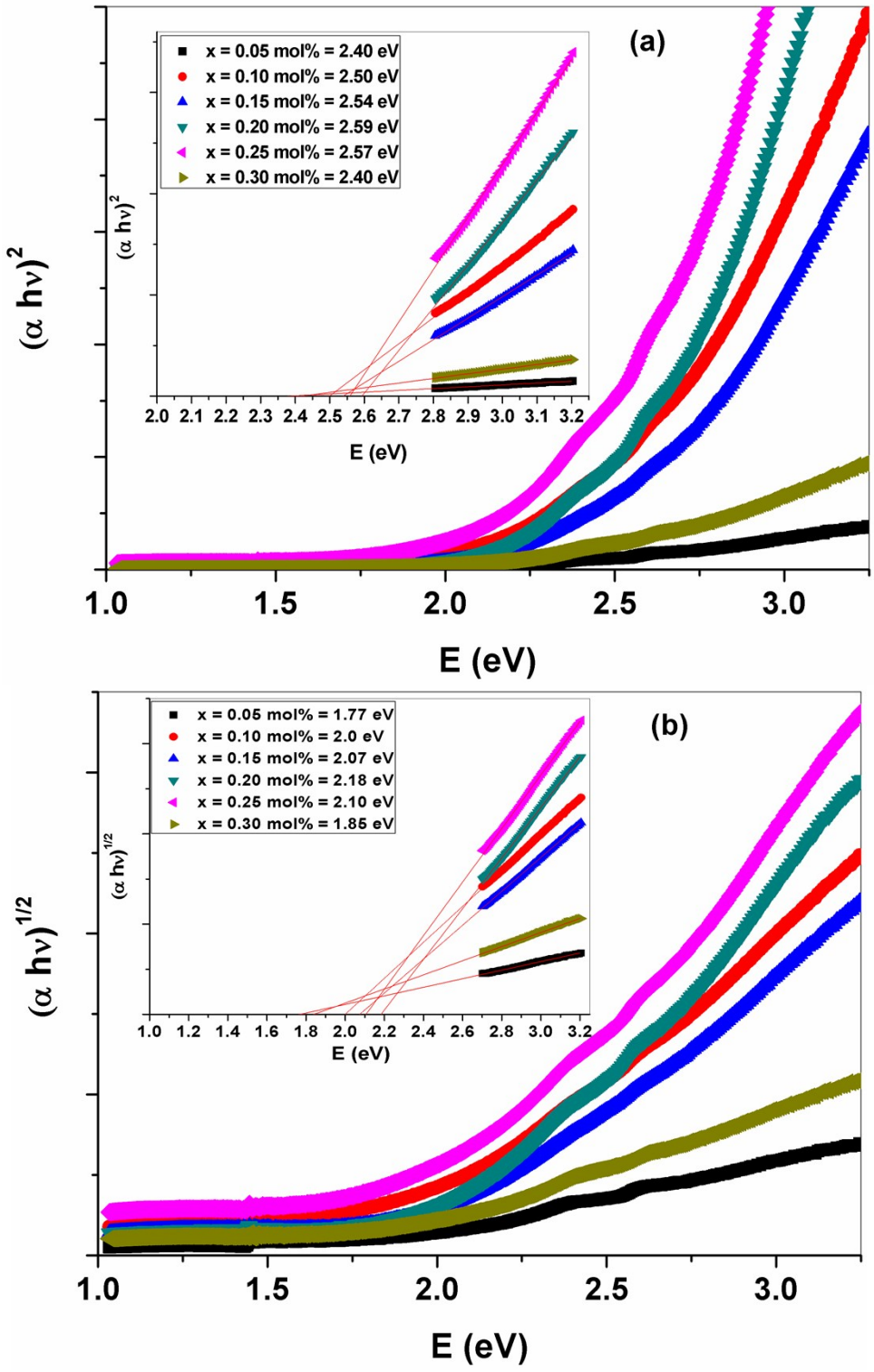

Figure S6. Direct (a) and indirect (b) band gap of cobalt doped iron sulphide $Co_xFe_{1-x}S_2$ thin films deposited from complexes (1) and (2) at 350 °C on glass substrate synthesised by AACVD with different starting ratio of cobalt complex (2).

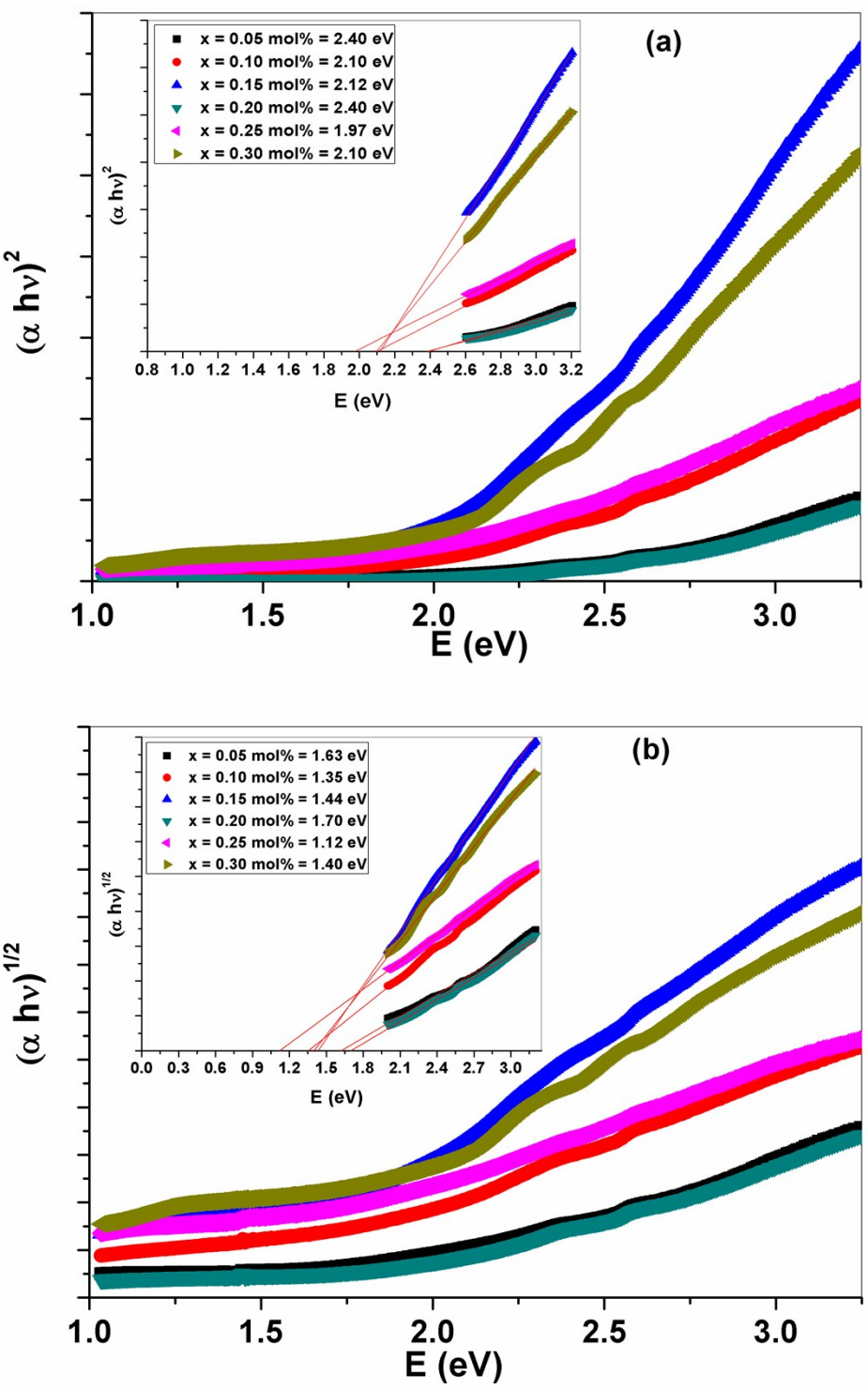

Figure S7. Direct (a) and indirect (b) band gap of nickel doped iron sulphide $Ni_xFe_{1-x}S_2$ thin films deposited from complexes (1) and (3) at 350 °C on glass substrate synthesized by AACVD with different starting ratio of nickel complex (3).

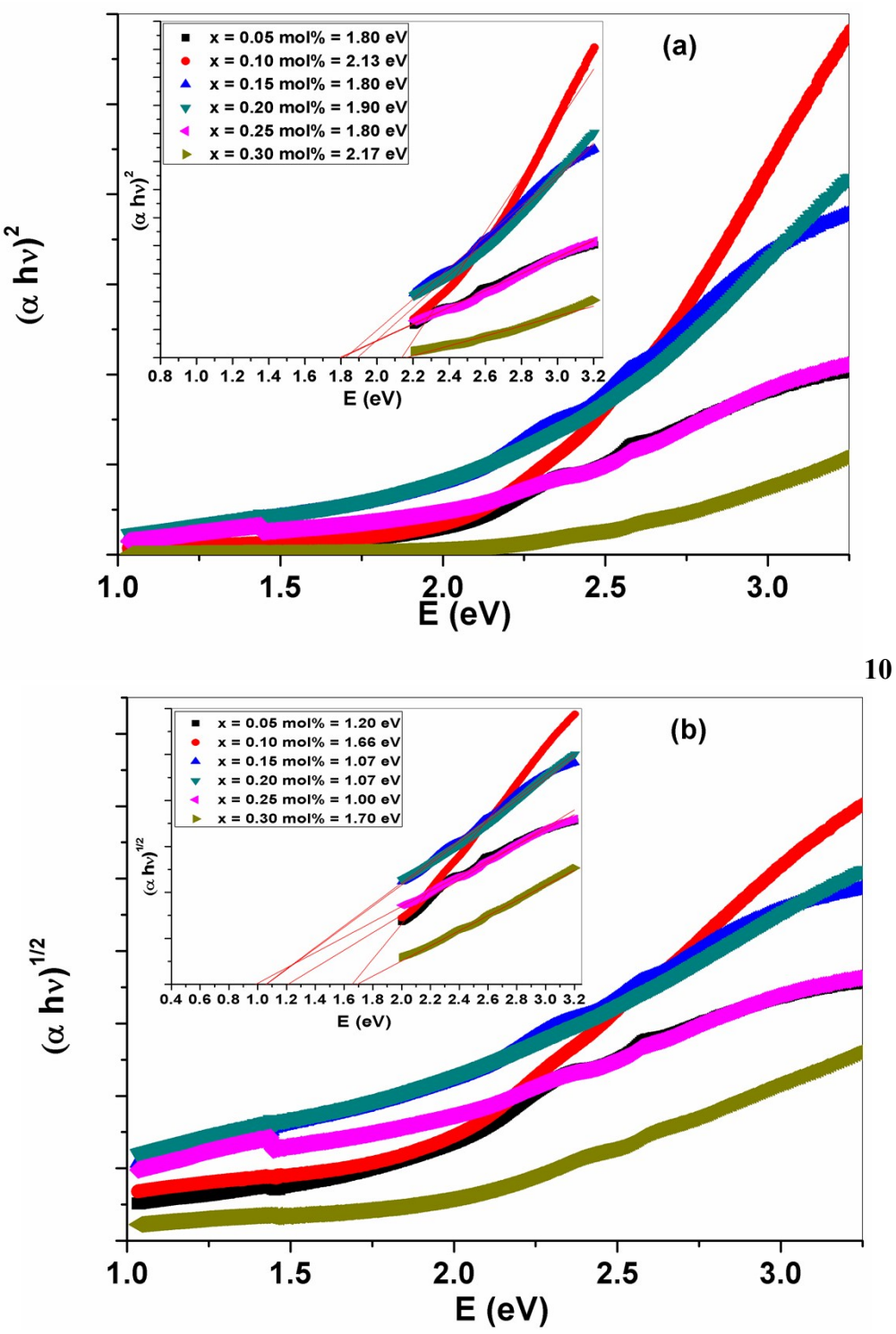

Figure S8. Direct (a) and indirect (b) band gap of copper doped iron sulphide $Cu_xFe_{1-x}S_2$ thin films deposited from complexes (1) and (4) at 350 °C on glass substrate synthesized by AACVD with different starting ratio of copper complex (4).

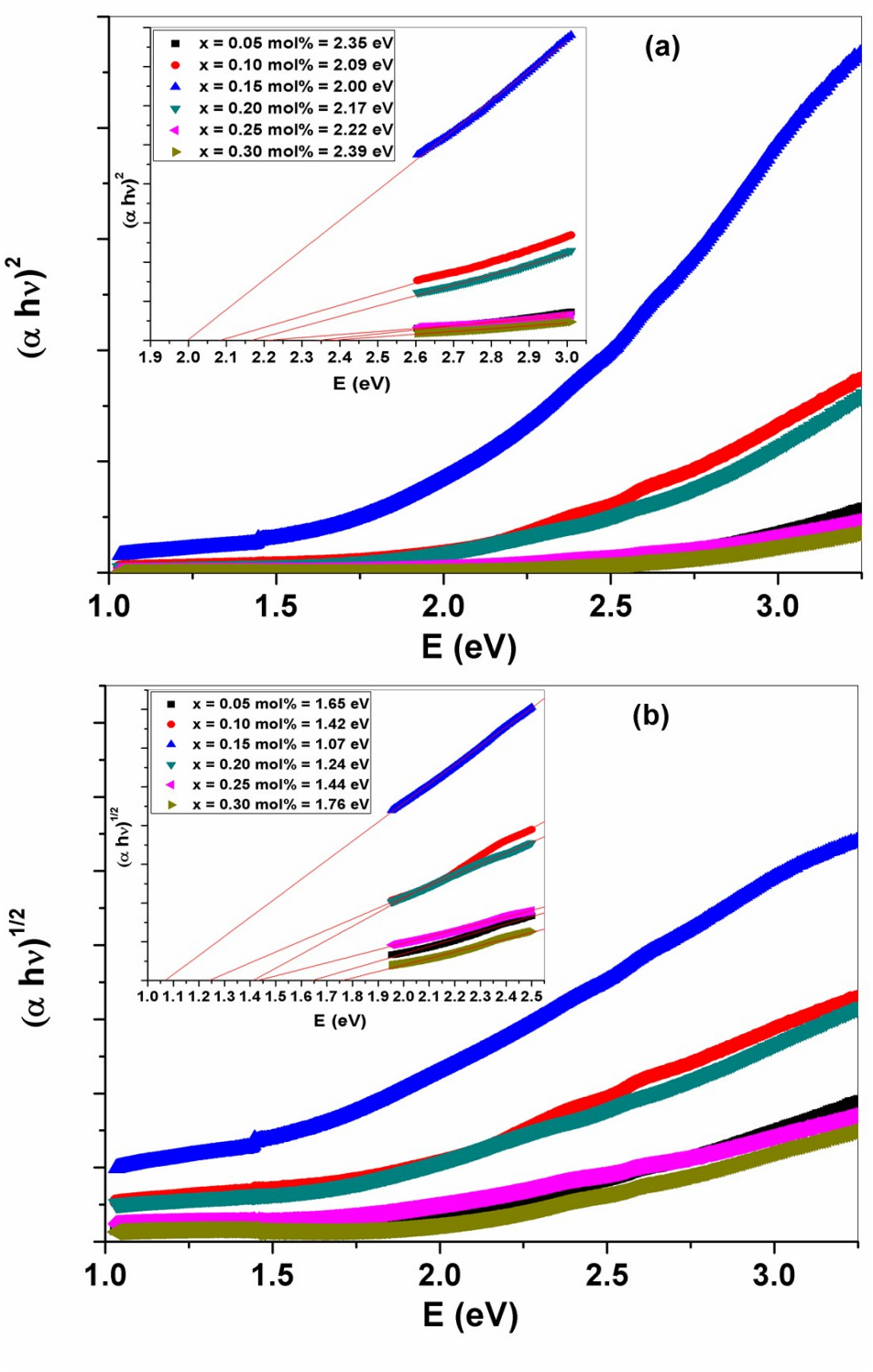

Figure S9. Direct (a) and indirect (b) band gap of zinc doped iron sulphide $Zn_xFe_{1-x}S_2$ thin films deposited from complexes (1) and (5) at 350 °C on glass substrate synthesized by AACVD with different starting ratio of zinc complex (5).

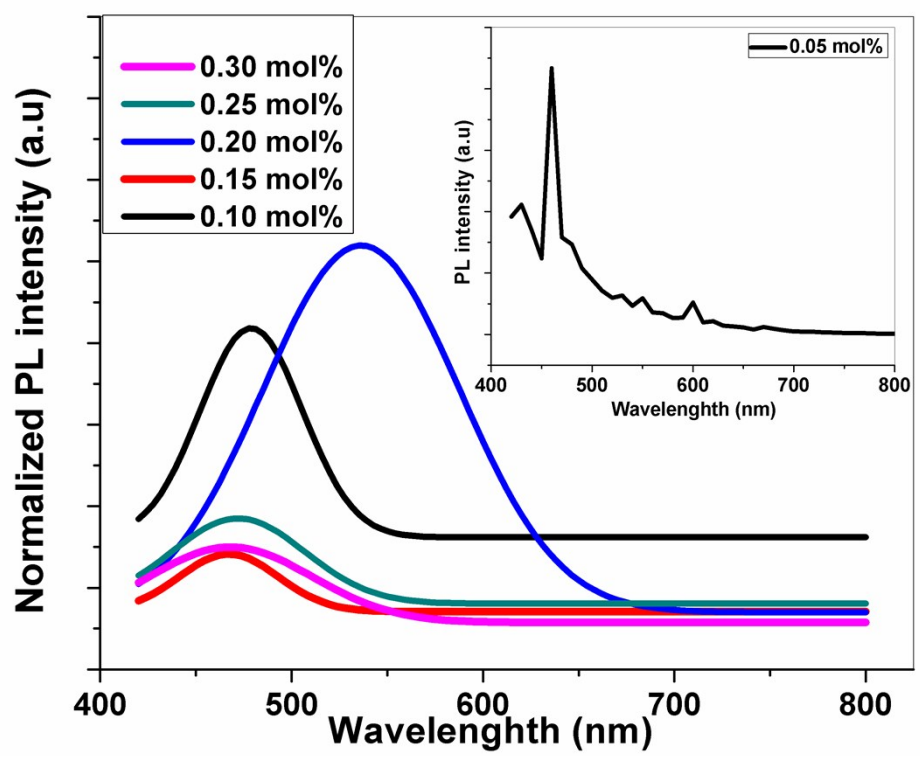

Figure S10. PL (Photoluminescence) spectra of cobalt doped iron sulphide $Co_xFe_{1-x}S_2$ thin films deposited from complexes (1) and (2) at 350 °C on glass substrate synthesised by AACVD with different starting ratio of cobalt complex (2).

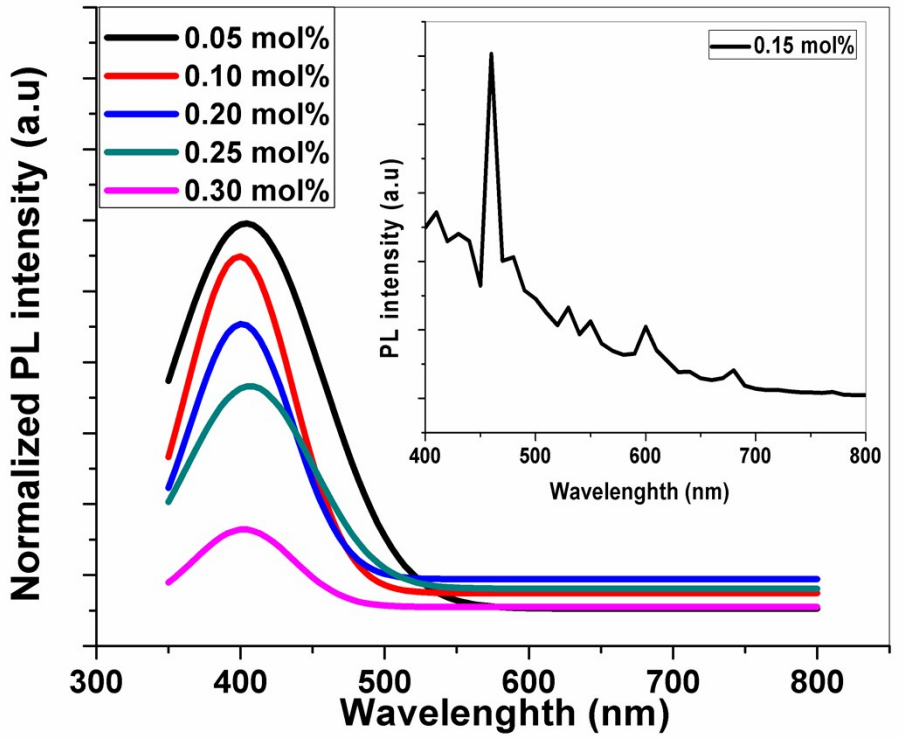

Figure S11. PL (Photoluminescence) spectra of nickel doped iron sulphide $Ni_xFe_{1-x}S_2$ thin films deposited from complexes (1) and (3) at 350 °C on glass substrate synthesized by AACVD with different starting ratio of nickel complex (3).

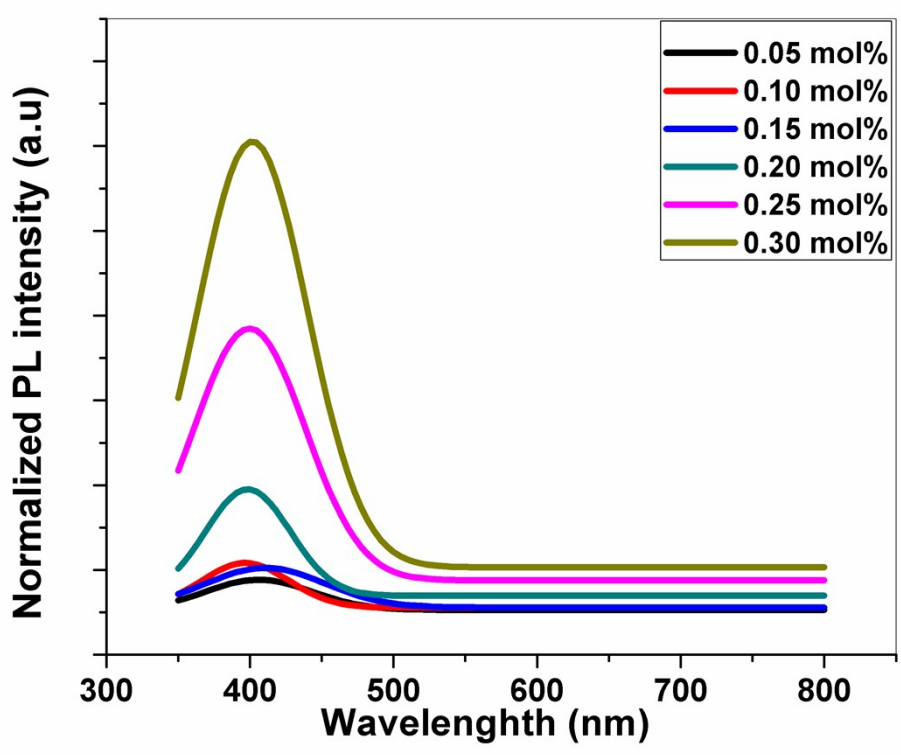

Figure S12. PL (Photoluminescence) spectra of copper doped iron sulphide $Cu_xFe_{1-x}S_2$ thin films deposited from complexes (1) and (4) at 350 °C on glass substrate synthesized by AACVD with different starting ratio of copper complex (4).

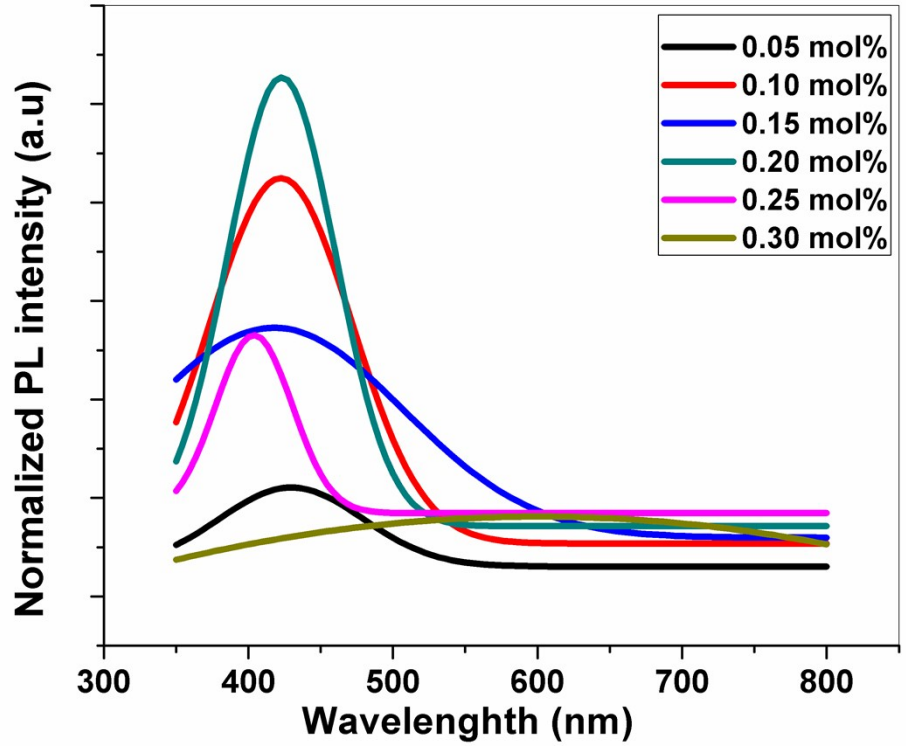

Figure S13. PL (Photoluminescence) spectra of zinc doped iron sulphide $Zn_xFe_{1-x}S_2$ thin films deposited from complexes (1) and (5) at 350 °C on glass substrate synthesized by AACVD with different starting ratio of zinc complex (5).